

Learning Extended Body Schemas from Visual Keypoints for Object Manipulation

Sarah Bechtel^{1,2}, Neha Das¹ and Franziska Meier¹

Abstract—Humans have impressive generalization capabilities when it comes to manipulating objects and tools in completely novel environments. These capabilities are, at least partially, a result of humans having internal models of their bodies and any grasped object. How to learn such body schemas for robots remains an open problem. In this work, we develop an approach that can extend a robot’s kinematic model when grasping an object from visual latent representations. Our framework comprises two components: 1) a structured keypoint detector, which fuses proprioception and vision to predict visual key points on an object; 2) Learning an adaptation of the kinematic chain by regressing virtual joints from the predicted key points. Our evaluation shows that our approach learns to consistently predict visual keypoints on objects, and can easily adapt a kinematic chain to the object grasped in various configurations, from a few seconds of data. Finally we show that this extended kinematic chain lends itself for object manipulation tasks such as placing a grasped object.

I. INTRODUCTION

Humans have impressive generalization capabilities when it comes to manipulating objects and tools. These capabilities are, at least partially, a result of humans having internal models of their bodies [1] which enables them to predict the consequences of their actions. Endowing robots with similar capabilities remains an important open research problem.

In this work, we consider the problem of learning predictive models from both visual and proprioceptive measurements, for model-based control of objects. We utilize keypoint representations which have been shown to be successful at capturing task-independent visual landmarks for various applications [2], [3]. Benefits of such learned representations over more traditional object representations (such as 6D pose), are the ability to represent non-rigid objects, and not requiring object models. In contrast to other learned latent-state representations, keypoints are interpretable, and are less prone to become task-dependent. However, the question of how a robot can manipulate objects through keypoint representations remains an open challenging problem.

Current state-of-the-art trains predictive action-conditioned models over keypoints [2], [4]. Once a dynamics model is trained, the robot can optimize actions to move observed keypoints into a desired goal configuration. However, these dynamics models are represented by unstructured neural networks, which tend to not extrapolate well to observations outside of the training distribution. This is compounded by the fact that learned visual keypoints may not consistently track the same part of the object throughout

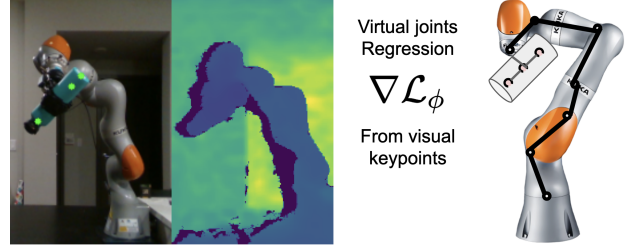


Fig. 1: Illustration: We learn an extended kinematic chain from visual keypoints and depth values. We introduce virtual joints to represent the object in the manipulators hand and learn the translation parameters of each virtual joint from visual features.

motion sequences, or may not track the object at all. As a result, such predictive models often do not perform well when used for object manipulation tasks.

We address these challenges as follows: First, during keypoint training, we encourage keypoint learning around the end-effector location, which leads to more consistent on-object keypoints. Then, instead of learning unstructured predictive models, we extend an existing kinematic model of the robots arm with virtual links and estimate the translation parameters of the links from visual keypoint predictions (see Figure 1). A key-feature of this step is that we can estimate parameters to adapt to various grasp variations of the object. Once the parameters of the virtual joints have been regressed, we have a fully differentiable forward kinematics model that can be utilized for model-based control.

To summarize, our contributions are as follows: 1) We extend the self-supervised learning approach for keypoint training presented in [2] by including proprioceptive state-measurements to spatially bias the visual keypoints around the end-effector. 2) We use a fully differentiable kinematic representation of the manipulator that we extended with learned virtual joints representing the object. We propose to perform gradient descent on the virtual joints given visual keypoint predictions as targets, to recover virtual joints parameters. We evaluate both contributions on a 7DoF iiwa Kuka arm, in simulation and on hardware. Our results show that when trained with proprioceptive information, the learned keypoints represent the manipulated objects more reliably. Furthermore, after regressing the virtual joints from visual information, we compare the resulting extended kinematic model to learned dynamics models on a model-based control task: placing a grasped object. Our method outperforms the learned dynamics models by an order of magnitude.

¹Facebook AI Research, Menlo Park, CA

²Max Planck Institute for Intelligent Systems, Tübingen, Germany
sbechtel@tuebingen.mpg.de

II. PROBLEM SETTING AND RELATED WORK

In this work we address deterministic, fixed-horizon and discrete time control tasks with continuous states $\mathbf{s} = (s_1, \dots, s_T)$ and continuous actions $\mathbf{u} = (u_1, \dots, u_T)$. Each state $s_t = [\theta_t, z_t]$ is the concatenation of the measured joint angles θ_t and a learned visual latent state z_t at time step t . The control tasks are characterized by a learned visual predictive model $\hat{s}_{t+1} = f(s_t, u_t)$ and a cost function $C(z_t, z_{\text{goal}})$ that measures the distance between current and desired goal state in visual latent space.

A. Learning visual predictive models and visual MPC

Our work is concerned with learning representations for robotic object manipulation. Here, we contrast our work to relevant approaches with respect to latent space representation, dynamics model learning and action optimization. Model-predictive control in visual space can be distinguished by how much, and what kind of structure is infused into the learning process. Approaches such as [5], utilize no structure and learn a predictive model f directly in pixel space. In contrast [6], [7], [2], [3], [8], [4] learn latent representations z by infusing various structural biases into their architectures, and then learn a predictive model f in the latent space, where f is parametrized via unstructured neural networks. Given a learned f , actions u are optimized via the cross-entropy method CEM [9], [5], [8], gradient based optimization [6], [4], or by using optimal control methods [7].

B. Fusing Vision and Proprioception

Most of the works above either do not utilize proprioceptive measurements, or only utilize them to train predictive models. We use proprioception to learn a better latent representation. Fusing vision and proprioception for better state-estimation is common in the rigid-body tracking literature [10], [11], [12] and has also recently been shown to lead to better learned state representations [13]. In our work we utilize proprioception to learn more relevant visual keypoints and learn an extended kinematic chain from them.

C. Learning body schemas

A promising alternative to unstructured predictive models are approaches that learn body schemas [1]: a model of a robots body and grasped objects or tools, which can then be used for control. Body schema approaches can be classified into approaches that estimate parameters of structured representations of a body and tool (i.e kinematic representation) [14], [15], [16], [17], [18], [19], or of unstructured models, such as neural network representations [20], [21], [22], [23], [24], [25]. To address the challenge of learning generalizable models, we follow approaches that learn parametrized kinematic models of a robot. Prior work in this category, typically utilizes markers or ground truth knowledge about the end-effector or tool-tip location in the robots workspace [14], [15], [16], [18] or simplified visual signals [17], and instead focus on the learning of the kinematic parameters. In contrast, our work extends an existing kinematic chain to include a grasped object, from learned visual latent representations.

III. BODY SCHEMA EXTENSION THROUGH KEYPOINTS

In this section we are going to explain 1) our approach for including structured kinematic information when training a visual keypoint detector, 2) how this enables us to learn an extended kinematic chain that includes the object in the manipulator's hand and 3) how the extended kinematic chain can be used for model-based control.

As already pointed out in section II, an object or a tool in the gripper of a manipulator can be seen as an extension of the kinematic chain of the robot. In Fig. 1, we visually show how the extension of the kinematic chain looks like for the kuka manipulator: additional virtual links and joints are added, representing the object in the manipulator's hand, to create a full chain that includes the object. The extended kinematics of the robot can then be controlled.

In order to train this extended body schema from vision, we first fuse visual and proprioceptive information of the robot to detect visual features of the object in the gripper. To this end we introduce a structured version of the keypoint detector presented in [2], that leverages proprioceptive information. The visual information about the object is then used to regress the kinematic parameters of the extended body schema.

A. Compute forward kinematics to image space

We specify $s_n^{\text{img}} = h^n(\theta)$ as a forward kinematic function, that directly projects the 3D position of link n in to image space when the robot is in configuration θ . To retrieve s_n^{img} , first the robots forward kinematic model is used to deliver x_n , the 3D location of link n in the robot's coordinate frame. Then x_n is projected into image and depth space. The full transformation is given by

$$s_n^{\text{img,depth}} = h^n(\theta) = T_{\text{proj}} T_{\text{cam}} x_n \text{ where } x_n = \prod_{i=1}^n T_i(\theta_i; \phi_i)$$

where T_i is the transformation matrix from the coordinate frame of link i to link $i-1$ and ϕ_i are the parameters (rotation and translation) of link i ; T_{cam} transforms x_n from robot to camera coordinate frame, and T_{proj} performs the projection to image and depth space. In the following, we will use $s_n^{\text{img,depth}}$ to denote the use of both image and depth value, and s_n^{img} when we only use image pixel predictions.

We assume that the parameters ϕ_i up to the end-effector index $n = \text{ee}$ are known, and we will use $h^{\text{ee}}(\theta)$ to combine visual and proprioceptive information to train a keypoint detector. Then we show how we can estimate the open parameters $\phi_{i>n}$, of virtual links, from visual keypoints.

B. Utilizing proprioception to learn object keypoints

In order to spatially bias keypoint learning to be close to end-effector location, we include proprioceptive information during training. Similar to the unstructured keypoint detector [2] we extract K 2-D visual feature maps o_k^{visual} (Fig.2) through a mini-RESNET 18, where K is the number of keypoints.

In this work, we propose to include proprioceptive information by computing a second feature map, which we

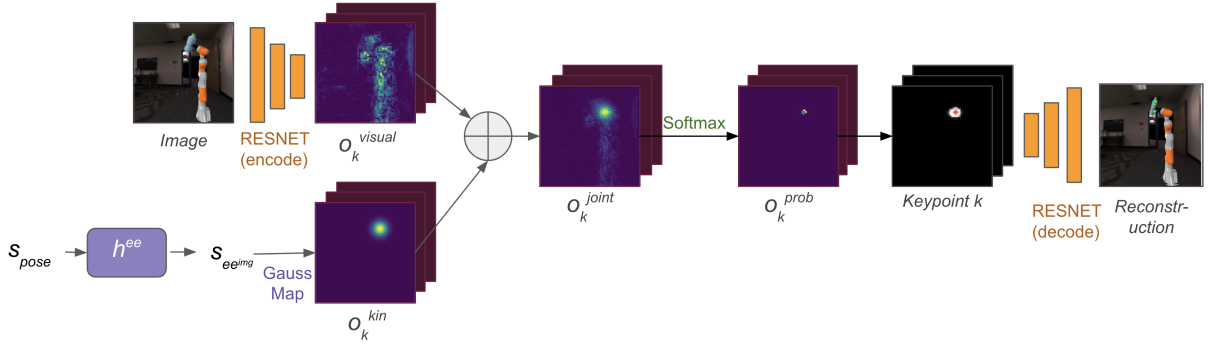


Fig. 2: Structured Keypoint Detector, fusing vision and proprioception. The forward kinematic model of the robot is used, to create a kinematic features map. The visual and the kinematic feature maps are then combined to train the keypoint detector.

call the kinematic feature-map o_k^{kin} , visible in Fig.2. The kinematic feature-map is generated by first computing the end-effector position in image space, $s_{ee}^{img} = h^{ee}(\theta)$, followed by placing a Gaussian blob g^{kin} over the location of the projected end-effector position in image space:

$$o_k^{kin} = g^{kin}(s_{ee}^{img})$$

where g^{kin} converts the pixel coordinates of s_{ee}^{img} into a heatmap with a Gaussian shaped blob $\mathcal{N}(s_{ee}^{img}, \Sigma)$ centered at x, y pixel locations of s_{ee}^{img} .

We then combine the kinematic with the visual feature map, creating a joint feature-map $o_k^{joint} = o_k^{visual} + o_k^{kin}$, which fuses visual and proprioceptive information. Given o_k^{joint} , keypoints are trained through a reconstruction objective, similar to the method presented in [2]. Figure 2 provides an overview of our adapted encoder-decoder architecture.

In [2], the loss is composed of a reconstruction error, a keypoint sparsity error, and a keypoint separation loss, that encourages to push keypoints apart. We propose to also include a loss that penalizes the distance between keypoints and end-effector. This *kinematic consistency loss*, together with the kinematic information during feature map creation, spatially biases the keypoint learning towards the end-effector location. The kinematic consistency loss, is given by

$$\mathcal{L}_{kin} = \sum_k (z_k^{[x,y,depth]} - s_{ee}^{img,depth})^2 \quad (1)$$

where $z_k^{[x,y,depth]}$ is the x, y pixel locations and depth value of the predicted keypoint z_k . The depth value of z_k is retrieved, by querying the depth image at pixel locations x, y .

C. Estimating virtual joints from visual keypoints

Once the keypoint detector has been trained, we use its predictions to learn an extension of the kinematic chain to include the object into the body schema. We extend the kinematics model from Section III-A, to include virtual links, one per visual keypoint, such that $s_k^{img,depth} = h_\phi^k(\theta)$ is the projection of the virtual links in image space. Here, ϕ are the learnable translation parameters of the virtual joints, that we aim to learn such that they represent the object (see Figure 1). To regress ϕ , a dataset $\mathcal{D} = \{(x_t = \theta_t, y_t = z_t)\}_{t=1}^T$ is collected where the trained keypoint detector is used to

predict visual $z^{[x,y,depth]}$ on images of the robot in joint configuration θ . The goal of this learning problem is to regress the translations ϕ , such that the output of $h_\phi^k(\theta)$ matches the keypoints detected by the detector. In other words, to optimize ϕ we want to minimize the loss \mathcal{L}_{trans} via gradient descent.

$$\mathcal{L}_{trans} = (s_k^{img,depth} - z^{[x,y,depth]})^2 \quad (2)$$

where $s_k^{img,depth} = h_\phi^k(\theta)$. This loss is a function of the learnable kinematic parameters ϕ , making it possible to update ϕ via gradient descent. Learning the translation parameters of the virtual joints, results in a new extended kinematic model, which includes the object. This new kinematic chain does not require visual information anymore and can be used for action optimization.

D. Gradient-Based Control for Object Manipulation

In contrast to other visual MPC work [5], [6], [4], that utilize learned visual dynamics models to optimize actions \mathbf{u} , we make use of the extended kinematic chain. Specifically, we define a visual predictive model $s_{t+1} = f(s_t, u_t)$ where $s_{t+1} = [\theta_{t+1}, z_{t+1}]$, and

$$\hat{\theta}_{t+1} = \theta_t + u_t \quad (3)$$

$$\hat{z}_{t+1} = h_\phi^k(\theta_{t+1}) \quad (4)$$

where actions \mathbf{u}_t are desired changes in joint positions. To optimize actions, we follow the gradient based action optimization presented in [6], [4] and minimize a task specific cost function C . Specifically, to optimize a sequence of action parameters $\mathbf{u} = (u_0, u_1, \dots, u_T)$ for a horizon of T time steps, we first predict the trajectory $\hat{\tau}$, that is created using an initial \mathbf{u} from starting configuration s_0 : $\hat{s}_1 = f(s_0, u_0)$, $\hat{s}_2 = f(s_1, u_1)$, \dots $\hat{s}_T = f(s_{T-1}, u_{T-1})$, which generates a predicted (or planned) trajectory $\hat{\tau}$. Intuitively, this step uses the extended kinematics model $h_\phi^n(\theta)$ to simulate forward what would happen if we applied action sequence \mathbf{u} to the initial state s_0 . We then measure the cost achieved $C(\hat{\tau}, z_{goal})$, where z_{goal} is a goal location in the visual domain. Since h is differentiable, the cost of the planned trajectory can be minimized via gradient descent.

$$\mathbf{u}_{new} = \mathbf{u} - \eta \nabla_{\mathbf{u}} C(\hat{\tau}, z_{goal}) \quad (5)$$

Details of our visual MPC algorithm can be found in [4].

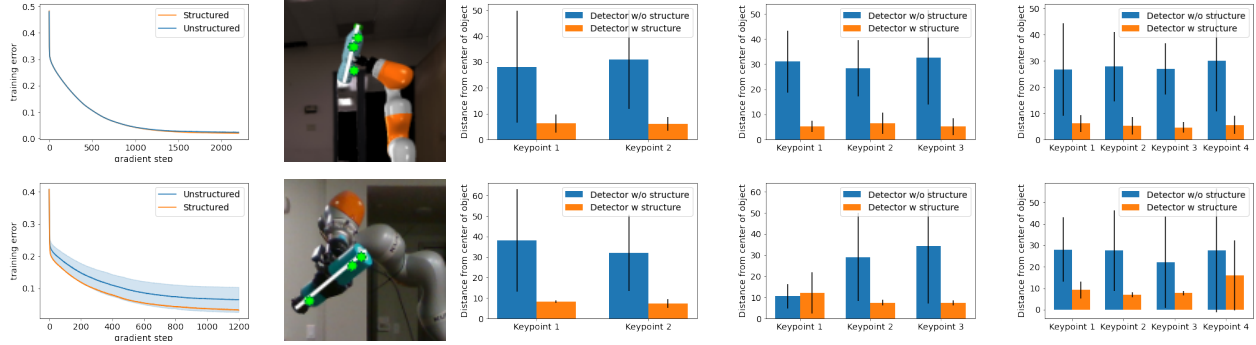


Fig. 3: **(top)** simulation results; **(bottom)** hardware results. **(1st col)** training loss for detector training, both detectors converge during training. **(2nd col)** illustration of evaluation metric. **(3rd to 5th col)** Results for training keypoint detectors with $K = 2, 3, 4$ keypoints, respectively. The bar plots show the average distance for each keypoint in pixel space. The structured keypoint detector (orange) predicts keypoints that are closer to the center line, and the average pixel distance suggests that they are placed on the object.

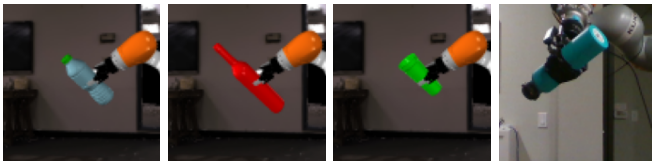


Fig. 4: The 3 objects used for simulation experiments, and one object on hardware.

IV. EXPERIMENTS

In this section we are going to present the experimental evaluation of our approach. We train two versions of the keypoint detector, one with kinematic structure, following the approach presented in section III, and one without kinematic structure, which is the detector presented in [26], as a comparison. All of our experiments are performed on a 7 DoF iiwa kuka arm [27], with an object attached to the kuka’s gripper. We present experiments in simulation and on hardware. For our simulation experiments we use the Habitat simulator [28] with a pybullet integration [29]. In simulation we use three different objects to show the adaptability of our approach. The experimental setup together with the objects used, is shown in Fig. 4 for simulation and hardware.

A. Data Collection

The keypoint architecture as presented in [2] is built to learn keypoints that capture motion in video-sequences. Because we aim to learn keypoints on the object, we collect data that only has object motion, similar to [4]. Specifically, we first move the manipulator to a random joint configuration, then we keep the manipulator in its position and only move the end-effector for 6 seconds. In total we collect data for 60 different joint configurations at a frequency of 5Hz for a total of 5 seconds, for each object. We collect image data, which includes RGB and depth data, alongside with proprioceptive information about the joint positions. Data collection on hardware follows the same procedure, and as presented in [4]: we collect 50 sequences of motion data in which only the end-effector and object move, starting from a random joint configuration. Each sequence is 3 seconds long, and contains 10 data frames.

B. Keypoint Detector Training Evaluation

The purpose of this evaluation is to analyse how well the keypoint detectors place keypoints on the object. After training, we compare the performance of the structured and unstructured keypoint detectors. For our simulation experiments, we present results averaged over five seeds and 3 different objects, where we train a detector per object. On hardware the experiments are also averaged over five seeds and we present results for two to four keypoints on a single object. First, we show the training loss curves in Figure 3(left), averaged across seeds, objects and number of keypoints. In simulation the loss curves are very similar, we believe that this is due to the reconstruction loss being the biggest component of the total training loss. Since only the gripper and object moves, the reconstruction for most of the image works well, reducing the loss and resulting in low training error even if the keypoints are not placed on the object.

Next, we evaluate how well the learned keypoints capture moving object. To this end, we define an imaginary line, that cuts through the object in the middle and connects its extremities. A visualization of it is visible in Fig. 3 (2nd column). Computing the shortest distance of a keypoint $z_k = (x_k, y_k)$ to this line, will give us a good intuition of whether this keypoint lies on the object or not. We perform this evaluation, for training detectors with $K = 2, 3, 4$ number of keypoints. We evaluate the detectors on a test dataset with 250 datapoints, that was held out during training. The distance is computed in pixel space and we report the mean and the standard deviation of that distance.

In Figure 3 we show the averaged distance of each trained keypoint to the line, with error bars, after training. Results for the simulation experiments (top row) and hardware experiments (bottom row) are shown. The bar plots illustrate the distance of the detected keypoints to the center line. We see that the structured keypoint detector, that was trained with proprioceptive information, outperforms the unstructured detector. The low distance to the center line suggests that the structured detector places the keypoints on the object.

This is confirmed by the qualitative analysis in Fig. 5 where three examples are shown. The structured detector detects keypoints that are on the object (top row). This is not true for the unstructured detector, which often fails at detecting keypoints that lie on the object (bottom row).

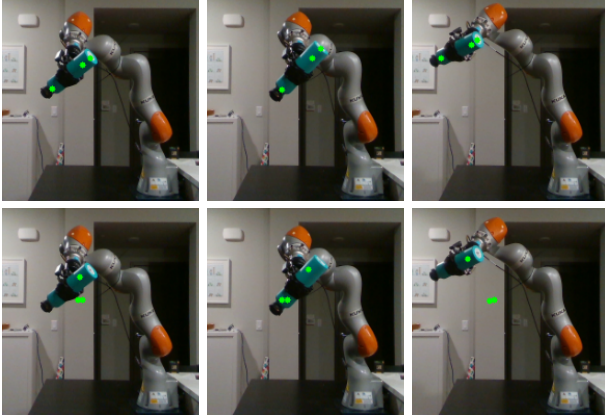


Fig. 5: Qualitative performance of structured (top) and baseline (bottom) keypoint detector on the hardware dataset. The structured keypoint detector, always detect keypoints on the object, this is not the case for the unstructured detector.

C. Virtual link/joint regression

We perform two set of experiments for the regression of virtual joint parameters: 1) to evaluate our virtual joint estimation procedure quantitatively, we test whether we can identify ground truth parameters $\bar{\phi}$, if we knew them; 2) We evaluate regressing virtual links from visual keypoints detected on 4 set of grasps.

To collect data for the first experiment, we pick a set of three ground truth virtual joint parameters $\bar{\phi}$ such that their projections $h_{\bar{\phi}}^k$ lie on the object. We collect a dataset $\mathcal{D} = \{(\theta_t, h_{\bar{\phi}}^k(\theta_t))\}_{t=1}^{15}$ for 15 random joint configurations θ . Then, we pretend to not know $\bar{\phi}$, initialize ϕ to be zero, and aim to estimate ϕ from the observations in \mathcal{D} via gradient descent, as described in Section III-C. In Fig.6, we show the MSE error between ground truth and estimated parameters $\|\phi - \bar{\phi}\|^2$ as a function of number of gradient steps, both from simulation and hardware data. We observe that after approximately 50 gradient steps ϕ converges towards their ground truth values, showing that the regression of virtual joint parameters from projected image and depth values is successful.

For our second set of experiments, we use the trained keypoint detectors to create a dataset $\mathcal{D} = \{(\theta_t, z_t)\}_{t=1}^{15}$, where z_t are the keypoints predicted by the detector, and learn virtual joints from these visual keypoint observations. The first image of Fig. 7 shows the visual keypoints predicted by the structured detector (in green), together with the projected virtual links h_{ϕ}^k (in red) after learning ϕ . The following two images show how the projection of the kinematic chain remains consistent, also when the pose θ of the manipulator changes. Results are presented for simulation (top) and on

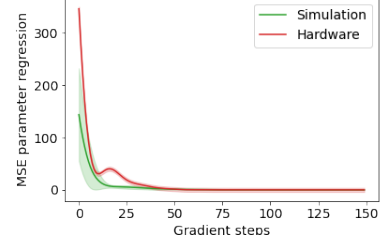


Fig. 6: Regression of kinematic parameters, MSE to ground truth virtual joint values over gradient steps. Our method is able to regress the virtual joint parameters successfully, on simulation and on hardware. Simulation results are averaged over five seeds and three object with manually chosen ground truth parameters for each object. Hardware results are averaged over five seeds.

hardware (bottom) experiments. The results show that we can successfully learn ϕ from visual features.

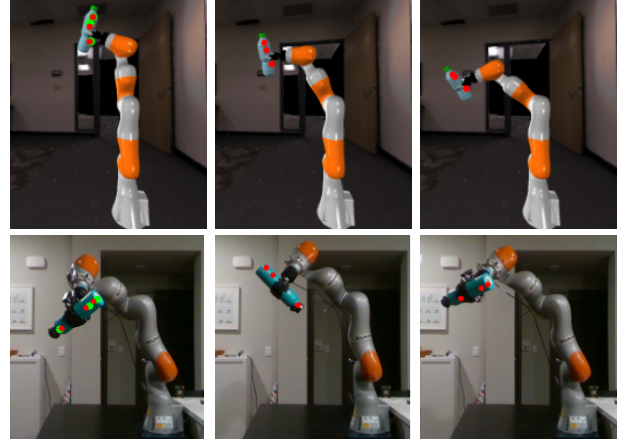


Fig. 7: Learned kinematic extension for three poses for simulation (top) and hardware (bottom). The first images shows, in green, the keypoints detected by the keypoint detector. The red dots are the projections in image given the learned virtual joints. Our method is able to successfully learn parameters ϕ , that generalize across poses.

Finally, we also evaluate our kinematic parameter regression when the robot re-grasps the object. Re-grasping changes the kinematic chain, by for example shifting it. In Fig. 8, we show how our method can successfully learn kinematic parameters ϕ that reflect this change. We show results for three new grasps. In the next section we present results for a downstream placing task, where our learned extended kinematic model is used, with different grasps, to place the object on a table.

D. Model-based Control for Object Manipulation

Finally, we compare our structured keypoint approach to various baselines on a object manipulation task, specifically a placing task (see Figure 9). During the placing task, the robot is required to manipulate the object in the gripper such that it successfully places it on a table. The actions are optimized for a time-horizon of $T = 10$ time steps, with the gradient based approach introduced in section III-D. We

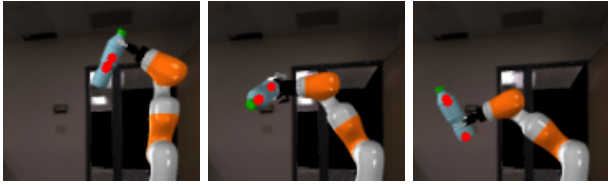


Fig. 8: Re-grasping for three different grasps. After each new grasp we regress the kinematic parameters successfully.

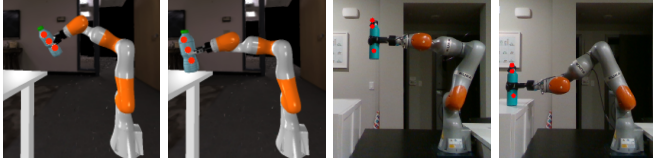


Fig. 9: Placing task in simulation and hardware

manually tune the cost function, which penalizes the distance between predicted and goal keypoint locations. This set of experiments show the applicability of our learned kinematic chain for a manipulation task. Furthermore, we compare to learned unstructured dynamics models.

We perform experiments in simulation and on hardware. Our approach learns an extended kinematic chain from the structured visual keypoints detector, that used proprioceptive information during training (see section III). The virtual joints, that represent the object, are regressed from a few measurements, as we described previously. Specifically we used three keypoints and thus, regress the parameters of three virtual joints. We compare our approach to the following four baselines that learn a dynamics model in the keypoint latent space:

a) *DynModel in 2D Keypoint space*: We train a keypoint detector as described in [2], [4] and train a dynamics model from data collected in a self-supervised fashion as described in [4].

b) *DynModel in 3D Keypoint space*: This baseline extends the one from above by including also depth information during training.

c) *DynModel in 2D-structured keypoint space*: We train a structured keypoint detector as described in section III-B, and then train a dynamics model in that space, instead of regressing virtual joint parameter.

d) *DynModel in 3D-structured keypoint space*: same as above, but here again we include depth.

For all our baselines we train a visual dynamics model in the keypoint space. We use dataset $\mathcal{D} = \{(\theta_t, u_t, z_t)\}_{t=0}^{2000}$ collected on sine motions of the robot, where z are the keypoints predicted by the detectors, to train a feedforward neural network. All the dynamics models are trained to convergences on the training data, and achieve a normalized mean squared error below 0.1 on the test data.

In Table I we report the results for our experiments. The simulation experiments are averaged over five seeds, the three objects introduced earlier and four different grasp positions. The results show the final distance of the object keypoints in the manipulators hand to the desired goal keypoints on the table. We perform a total of three tasks

that vary in start-goal configurations. All the distances are reported in pixel space, and represents the root mean squared error (RMSE). Between all the baselines, the baselines c) and d) that use our proposed keypoint detector, perform best. This indicates, that the keypoints trained with our detector are better suited for the object manipulation task. Yet overall, compared to our extended kinematic chain, all of them perform fairly poorly in the model-based control task. Our approach outperforms all baseline variations and is the only one to successfully place the object on the table. This gap in performance can be explained by the fact that the extended kinematic is able to generalize throughout the state-space, while the trained dynamics models prediction quality deteriorates quickly outside of the training data distribution.

It is worthwhile noting, that our approach is successful also when used on the real robot, where we achieve an average RMSE of 3.92 pixels. This is remarkable not only because on hardware noise and controller inaccuracies often make the task harder, but also because we run our optimized action sequence in a feedforward fashion, without having to replan at each time step.

Method	Task 1 Mean (Std)	Task 2 Mean (Std)	Task 3 Mean (Std)
Ours	4.85(2.91)	2.04(1.26)	2.06(1.18)
a	155.62(343.84)	60.78(73.67)	70.00(67.73)
b	135.16(119.7)	69.60(59.69)	85.32(83.27)
c	103.35(85.07)	29.37(48.09)	70.38(88.42)
d	120.21(107.39)	40.14(42.95)	96.58(258.14)
Hardware	4.06 (3.83)	2.12 (0.04)	5.60 (4.43)

TABLE I: The performance of three placing tasks. We compare our method to the baselines introduced before. We report the final distance of the object in the hand from the desired target position of the object as root mean squared error. We average our results over five seeds and four different re-grasps of the object in simulation. On hardware we average over five seeds. The errors are reported in pixel space.

V. CONCLUSION

We present a method for learning extended body schemas from vision, that incorporates an object in the manipulator’s hand. We show how merging proprioceptive information and vision enables us to learn better visual latent representation of the object, which can be used to successfully learn an extension of a robots kinematics model. Specifically the learned extended kinematic chain, incorporates the object into the kinematic model of the robot. We show how we can use the learned kinematic model for object manipulation on a placing task and how we can adapt the kinematic chain for different grasps. Our experiments on a 7 DoF iiwa kuka arm in simulation and on hardware, show the generality of our approach and the good performance to out of distribution tasks. In the future we would like to explore more complex, contact rich manipulation tasks, that use the learned extended body schema to control the robot.

REFERENCES

- [1] M. Hoffmann, H. Marques, A. Arieta, H. Sumioka, M. Lungarella, and R. Pfeifer, "Body schema in robotics: a review," *IEEE Transactions on Autonomous Mental Development*, vol. 2, no. 4, pp. 304–324, 2010.
- [2] M. Minderer, C. Sun, R. Villegas, F. Cole, K. P. Murphy, and H. Lee, "Unsupervised learning of object structure and dynamics from videos," in *Advances in Neural Information Processing Systems*, 2019, pp. 92–102.
- [3] T. D. Kulkarni, A. Gupta, C. Ionescu, S. Borgeaud, M. Reynolds, A. Zisserman, and V. Mnih, "Unsupervised learning of object keypoints for perception and control," in *Advances in neural information processing systems*, 2019, pp. 10 724–10 734.
- [4] N. Das, S. Bechtel, T. Davchev, D. Jayaraman, A. Rai, and F. Meier, "Model-based inverse reinforcement learning from visual demonstrations," in *4th Conference on Robot Learning (CoRL)*. IEEE, 2020.
- [5] F. Ebert, C. Finn, S. Dasari, A. Xie, A. X. Lee, and S. Levine, "Visual foresight: Model-based deep reinforcement learning for vision-based robotic control," *CoRR*, vol. abs/1812.00568, 2018. [Online]. Available: <http://arxiv.org/abs/1812.00568>
- [6] A. Byravan, F. Leeb, F. Meier, and D. Fox, "Se3-pose-nets: Structured deep dynamics models for visuomotor control," in *2018 IEEE International Conference on Robotics and Automation (ICRA)*, 2018.
- [7] M. Watter, J. Springenberg, J. Boedecker, and M. Riedmiller, "Embed to control: A locally linear latent dynamics model for control from raw images," in *Advances in neural information processing systems*, 2015, pp. 2746–2754.
- [8] M. Lambeta, P. Chou, S. Tian, B. Yang, B. Maloon, V. R. Most, D. Stroud, R. Santos, A. Byagowi, G. Kammerer, D. Jayaraman, and R. Calandra, "Digit: A novel design for a low-cost compact high-resolution tactile sensor with application to in-hand manipulation," *IEEE Robotics and Automation Letters*, 2020.
- [9] R. Y. Rubinstein and D. P. Kroese, *The Cross Entropy Method: A Unified Approach To Combinatorial Optimization, Monte-Carlo Simulation (Information Science and Statistics)*. Berlin, Heidelberg: Springer-Verlag, 2004.
- [10] C. Garcia Cifuentes, J. Issac, M. Wüthrich, S. Schaal, and J. Bohg, "Probabilistic articulated real-time tracking for robot manipulation," *IEEE Robotics and Automation Letters*, 2017.
- [11] D. Kappler, F. Meier, J. Issac, J. Mainprice, C. G. Cifuentes, M. Wüthrich, V. Berenz, S. Schaal, N. Ratliff, and J. Bohg, "Real-time perception meets reactive motion generation," *IEEE Robotics and Automation Letters*, 2018.
- [12] R. Martín-Martín and O. Brock, "Cross-modal interpretation of multi-modal sensor streams in interactive perception based on coupled recursion," in *2017 IEEE/RSJ International Conference on Intelligent Robots and Systems (IROS)*. IEEE, 2017, pp. 3289–3295.
- [13] M. A. Lee, Y. Zhu, K. Srinivasan, P. Shah, S. Savarese, L. Fei-Fei, A. Garg, and J. Bohg, "Making sense of vision and touch: Self-supervised learning of multimodal representations for contact-rich tasks," in *2019 International Conference on Robotics and Automation (ICRA)*. IEEE, 2019, pp. 8943–8950.
- [14] J. Sturm, C. Plagemann, and W. Burgard, "Body schema learning for robotic manipulators from visual self-perception," *Journal of Physiology-Paris*, vol. 103, no. 3-5, pp. 220–231, 2009.
- [15] R. Martinez-Cantin, M. Lopes, and L. Montesano, "Body schema acquisition through active learning," in *2010 IEEE international conference on robotics and automation*. IEEE, 2010, pp. 1860–1866.
- [16] S. Ulbrich, V. R. de Angulo, T. Asfour, C. Torras, and R. Dillmann, "Rapid learning of humanoid body schemas with kinematic bézier maps," in *2009 9th IEEE-RAS International Conference on Humanoid Robots*. IEEE, 2009, pp. 431–438.
- [17] M. Hersch, E. Sauser, and A. Billard, "Online learning of the body schema," *International Journal of Humanoid Robotics*, 2008.
- [18] N. Gothoskar, M. Lázaro-Gredilla, A. Agarwal, Y. Bekiroglu, and D. George, "Learning a generative model for robot control using visual feedback," *arXiv preprint arXiv:2003.04474*, 2020.
- [19] K. Stepanova, T. Pajdla, and M. Hoffmann, "Robot self-calibration using multiple kinematic chains—a simulation study on the icub humanoid robot," *IEEE Robotics and Automation Letters*, vol. 4, no. 2, pp. 1900–1907, 2019.
- [20] B. Boots, A. Byravan, and D. Fox, "Learning predictive models of a depth camera & manipulator from raw execution traces," in *2014 IEEE International Conference on Robotics and Automation (ICRA)*. IEEE, 2014.
- [21] M. Hikita, S. Fuke, M. Ogino, T. Minato, and M. Asada, "Visual attention by saliency leads cross-modal body representation," in *2008 7th IEEE International Conference on Development and Learning*. IEEE, 2008, pp. 157–162.
- [22] M. Rolf, J. J. Steil, and M. Gienger, "Learning flexible full body kinematics for humanoid tool use," in *2010 International Conference on Emerging Security Technologies*. IEEE, 2010, pp. 171–176.
- [23] C. Nabeshima, Y. Kuniyoshi, and M. Lungarella, "Adaptive body schema for robotic tool-use," *Advanced Robotics*, vol. 20, no. 10, pp. 1105–1126, 2006.
- [24] Y. Yoshikawa, K. Hosoda, and M. Asada, "Does the invariance in multi-modalities represent the body scheme?—a case study with vision and proprioception," in *2nd Intelligent Symposium on Adaptive Motion of Animals and Machines*. Citeseer, 2003.
- [25] G. Schillaci, V. V. Hafner, and B. Lara, "Coupled inverse-forward models for action execution leading to tool-use in a humanoid robot," in *2012 7th ACM/IEEE International Conference on Human-Robot Interaction (HRI)*. IEEE, 2012, pp. 231–232.
- [26] L. Manuelli, W. Gao, P. Florence, and R. Tedrake, "kpam: Keypoint affordances for category-level robotic manipulation," *International Symposium on Robotics Research (ISRR)*, 2019.
- [27] K. AG. (2020) Kuka ag. [Online]. Available: <https://www.kuka.com>
- [28] Manolis Savva*, Abhishek Kadian*, Oleksandr Maksymets*, Y. Zhao, E. Wijmans, B. Jain, J. Straub, J. Liu, V. Koltun, J. Malik, D. Parikh, and D. Batra, "Habitat: A Platform for Embodied AI Research," in *Proceedings of the IEEE/CVF International Conference on Computer Vision (ICCV)*, 2019.
- [29] Erwin Coumans and Yunfei Bai, "Pybullet, a python module for physics simulation in robotics, games and machine learning." <http://pybullet.org/>, 2016–2019.